



## Critical energy release rates of weak snowpack layers determined in field experiments

Christian Sigrist<sup>1</sup> and Jürg Schweizer<sup>1</sup>

Received 26 October 2006; revised 21 December 2006; accepted 10 January 2007; published 15 February 2007.

[1] A field experiment was developed to measure the critical energy release rate for fracture propagation in a weak snowpack layer. A snow block was isolated on a slope and tested in-situ by cutting along the weak layer. Critical cut lengths of about 25 cm were required to start fracture propagation along the weak layer. The critical energy release rate was determined numerically from the critical cut length with a finite element simulation. The mean critical energy release rate for the tested weak layers was about 70 mJ m<sup>-2</sup>. Numerical simulations showed that slope normal bending of the slab, in addition to the slope parallel shear deformation, contributed considerably to the energy release rate in our experimental setup. **Citation:** Sigrist, C., and J. Schweizer (2007), Critical energy release rates of weak snowpack layers determined in field experiments, *Geophys. Res. Lett.*, 34, L03502, doi:10.1029/2006GL028576.

### 1. Introduction

[2] A dry-snow slab avalanche is released by a sequence of fracture processes in the snow cover [Schweizer *et al.*, 2003]. When a weak layer overlain by a cohesive slab is damaged over a certain area, a fracture spreads out along the plane of weakness followed by tensile fracture on the upper periphery. After the loss of peripheral support the slab is fully released, disintegrates and flows downslope. McClung [1979, 1981] has introduced a model of dry-snow slab release – based on the seminal work of Palmer and Rice [1973] – that expressed slope stability in terms of the mode II fracture toughness. Recently, Heierli and Zaiser [2006] proposed an analytical model on fracture nucleation in a collapsible stratification. They showed that the energy barrier for crack propagation can be considerably lowered by an additional slope normal collapse of the weak layer.

[3] The first measurements of fracture toughness (however in mode I) were performed by Kirchner *et al.* [2000]. Their work stimulated a number of laboratory and field studies [e.g., Failletaz *et al.*, 2002; Schweizer *et al.*, 2004; Sigrist *et al.*, 2005, 2006; Fyffe, 2006; Gauthier and Jamieson, 2006a, 2006b]. Most of the laboratory work focused on mode I fracture experiments with snow beams. Experimental results confirmed that snow has to be considered as a quasi-brittle material subjected to a considerable size effect [Sigrist *et al.*, 2005] as previously proposed by Bažant *et al.* [2003].

[4] A variety of field tests was developed that aimed to provide information on fracture propagation potential

[Gauthier and Jamieson, 2006a, 2006b; Simenhois and Birkeland, 2006]. Gauthier and Jamieson [2006a] were the first to report on a suitable design. Independently, we performed similar experiments and analysed the measurements based on fracture mechanics. The critical energy release rate  $G_c$ , a measure for the energy that is required to fracture a unit area of the weak layer, has to be exceeded by the energy released in a crack advance  $\Delta a$  in order to start a self-propagating fracture. The critical energy release rate is considered to be one of the key criteria to determine if fracture propagation is possible in the dry-snow slab avalanche release process.

### 2. Methods

#### 2.1. Field Test Setup

[5] A snow block with a width of 0.3 m and a variable length of 0.6 m, 1.2 m, or 1.8 m was isolated on all four sides on a slope by shovelling a ditch (Figure 1). After the weak layer had been identified by a separate compression test [Jamieson, 1999], a cut was made along the weak layer with a snow saw (thickness 2 mm) until the crack length became critical ( $a_c$ ) and self-propagation of the crack started. The cut was usually made from the top end in downslope direction (occasionally in upslope direction) with a rather slow (2–4 cm s<sup>-1</sup>) and smooth sawing movement.

#### 2.2. Finite Element Model of Field Test

[6] Since the available analytical solutions for a determination of the energy release rate  $G$  did not match our experimental setup, a finite element (FE) model of the experimental geometry was created. The total strain energy  $U(a)$  for a cut length  $a$ , and  $U(a + \Delta a)$  for a cut length  $a + \Delta a$  were calculated, where  $\Delta a$  is a small increase in the cut length. The energy release rate  $G$  was then calculated as the energy difference divided by the specimen thickness  $w$  and the cut length increment  $\Delta a$ :

$$G(a) = \frac{U(a + \Delta a) - U(a)}{w\Delta a} \quad (1)$$

Thereby,  $\Delta a$  was evaluated empirically by choosing it small enough for  $G(a)$  to converge but large enough to avoid errors due to the limited precision of the FE model. The critical energy release rate  $G_c$  was calculated according to  $G_c = G(a_c)$ . The model consisted of a basal layer which was fixed in  $x$  and  $y$  direction at the bottom (Figure 2a), overlain by a slab consisting of  $n$  layers (38'000 nodes in total). For our experiments the slab was modelled as to consist of three layers ( $n = 3$ ), corresponding to the distinguishable layers in a manually observed snow profile [Colbeck *et al.*, 1990]. However, the number of slab layers can easily be adjusted.

<sup>1</sup>WSL Swiss Federal Institute for Snow and Avalanche Research, Davos, Switzerland.

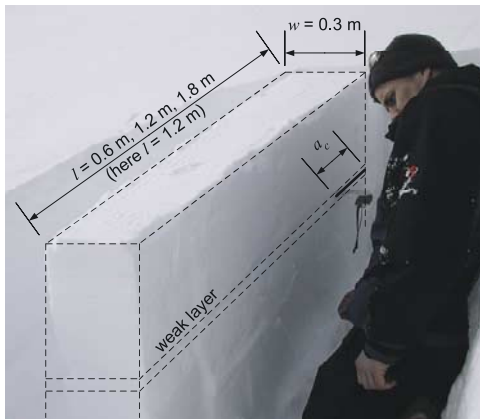


**Figure 1.** Experimental setup: cutting along the weak layer of an isolated snow block on a slope.

[7] The cut that was made with the snow saw was not only modelled in its length  $a_c$ , but also in its thickness of 2 mm, indicated as “gap” in Figure 2a. The cut surfaces were restricted from penetrating into each other, in case the two surfaces would get in contact due to bending.

[8] Each field test was modelled according to its specific geometry and snow properties. The following parameters were required as input for the model: length  $l$  and width  $w$  of the block, thickness, density and elastic properties (Young’s modulus  $E$  and Poisson’s ratio  $\nu$ ) of the different layers of the slab, as well as of the basal layer, cut length at failure  $a_c$ , and the slope angle  $\varphi$ . The Poisson’s ratio  $\nu$  was estimated from density according to  $\nu = \nu_0 + c(\rho - \rho_0)$ , with  $\nu_0 = 0.2$ ,  $\rho_0 = 300 \text{ kg m}^{-3}$  and  $c = 5 \times 10^{-4} \text{ m}^3 \text{ kg}^{-1}$  [Mellor, 1975]. The cut length increment  $\Delta a$  was set to 0.002 m. Since a variation of the weak layer properties did not change the FEM results, the weak layer itself was modelled as to consist of the same material as the adjacent upper slab. The Young’s modulus for each layer was determined via a penetration resistance profile acquired with a snow micropenetrometer (SMP) [Johnson and Schneebeli, 1999], since penetration resistance is related to the modulus [see Sigrist, 2006]. For the slab densities found in our field experiments, values of the Young’s modulus were in the range of 5 to 10 MPa.

[9] The influence of the cut thickness on the energy release rate  $G$  was analysed with a rectangular block model including a cut, once with a vertical extension of 2 mm (Figure 2b), and once with zero vertical extension (Figure 2c). In case of zero extension no slope normal bending of the slab was possible. Zero slope parallel friction between the cut surfaces was assumed. The energy release rate for the case without bending  $G_{shear}$  (gap = 0 mm) was then compared to the case with bending and shear deformation  $G_{tot}$  (gap = 2 mm). The rectangular shape, in contrast to the shape of the field experiment model (Figure 2a), was chosen to be able to model also high slope angles. The block model had the following dimensions: block length = 1.2 m, block width = 0.3 m, slab thickness = 0.3 m, thickness of basal layer = 0.1 m, cut length = 0.2 m.

### 3. Results

[10] Field experiments were performed during three days between 25 January and 3 February 2006. An east-facing

slope was selected with a slope angle close to  $30^\circ$  at Strela-Schönboden, Davos, Switzerland. In the snow cover a weak layer was present in a depth of about 30 cm which consisted of faceted crystals and partly depth hoar overlain by a 2 mm crust. Three test series were performed (33 experiments) with this weak layer at intervals of 2 and 7 days, respectively (Table 1).

#### 3.1. Types of Failure

[11] The test results can be divided in two groups according to their failure behaviour. The first type fractured along the entire weak layer plane of the snow block after a critical cut length  $a_c$  was reached. Because the experiments were performed at a slope angle of about  $30^\circ$ , the detached part of the block (slab) did not slide down, but a noticeable slope normal and slope parallel displacement of the whole slab of a few millimeters was observed. In the second type, a fracture propagated along the weak layer when reaching  $a_c$  but the weak layer did not fracture entirely. The crack was arrested after a certain distance. In some cases a vertical tensile crack through the overlying slab was observed. Similar failure types were observed by Gauthier and Jamieson [2006a]. In 22 out of 33 experiments, the weak layer fractured entirely, and in 11 tests the crack was arrested.

[12] Tests that were made on slopes steeper than  $30^\circ$  showed that the slab slid down over the plane of weakness.

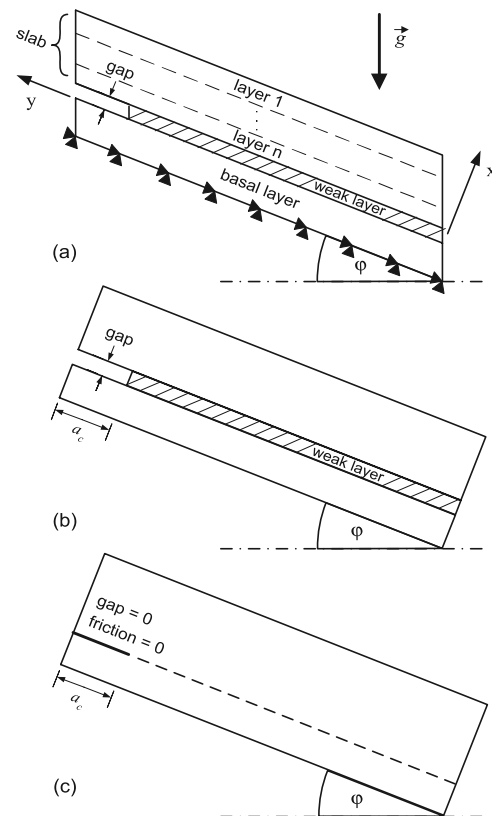


**Figure 2.** (a) Geometry of the FE model. Black triangles indicate the boundary conditions. Nodes are fixed in  $x$  and  $y$  direction. (b) FE model used to simulate the effect of a slope normal gap allowing slope normal bending of the slab and (c) FE model of a block with a gap with zero extension. Slope normal bending is restricted.

**Table 1.** Summary of Field Experiments<sup>a</sup>

Date of Testing	Number of Experiments	Snow Type of Weak Layer	Compression Test Results Number of Tabs (Rating)	Mean Slab Density, kg m <sup>-3</sup>	Mean Slab Thickness (Slope Normal), m	Mean Cut Length, $a_c \pm$ sdev, m	Snow/Air Temperature, °C
25 Jan 06	5 (4/1) <sup>b</sup>	Faceted crystals and partly depth hoar, 1–3 mm, F <sup>c</sup>	11, 11, 12 (moderate)	173	0.27	0.22 ± 0.03	–6.9/–3.2
27 Jan 06	21 (13/8) <sup>b</sup>	Faceted crystals and partly depth hoar, 1–2 mm, F <sup>c</sup>	13, 13; 13, 13; 14, 12; 13, 13; 15, 14; 15, 13 (moderate)	187	0.26	0.23 ± 0.02	–7.4/–9
3 Feb 06	7 (5/2) <sup>b</sup>	Faceted crystals and depth hoar, 1–2.5 mm, F <sup>c</sup>	14, 15; 15, 15; 16, 17; 17, 15, 15 (moderate)	202	0.21	0.25 ± 0.02	–6.3/–3.5

<sup>a</sup>Date of the field day and number of tests are given. Snow type is given as grain shape, grain size and hardness index according to ICSSG [Colbeck *et al.*, 1990].

<sup>b</sup>Number of test in which the beam failed completely/number of tests in which the crack was arrested.

<sup>c</sup>Hand hardness index: F = Fist.

Tests on slopes with inclinations as low as 13° confirmed that the field test worked also for slopes less steep than 30°. However, these tests were not considered because the tested weak layers were different to the ones discussed below.

**3.2. Critical Energy Release Rate for the Tested Weak Layer**

[13] SMP profiles were acquired only on 27 January 2006 and therefore only for this series  $G_c$  could be evaluated, as the modelling required the elastic properties of the different layers. Three different block length  $l$  were tested. The mean critical energy release rate  $G_c$  was found to be independent of  $l$  ( $N = 21, p = 0.31$ ). The mean critical energy release rate  $G_c$  was calculated to be  $G_c = 0.07 \pm 0.02 \text{ J m}^{-2}$ . The critical cut length  $a_c$  required for fracture propagation was  $a_c = 0.23 \pm 0.03 \text{ m}$ . Figure 3 shows that the critical cut length tended to increase with time. The load due to the slab did not increase during this period because there was no snow fall or wind drift event. However, the density did increase due to settlement of the slab layer (Table 1). The increase of the critical cut length coincided with an increase of the compression test (CT) score (Figure 3).

**3.3. Influence of Bending**

[14] FEM analysis showed that although the thickness of the cut was only 2 mm, the cut surfaces did not touch each other for our cut length ( $a_c < 0.3 \text{ m}$ ) and slab properties. In Figure 4 the ratio of the energy release rate due to slope parallel shear deformation  $G_{shear}$  to the energy release rate due to shear and bending of the slab  $G_{tot}$  is plotted in relation to the slope angle  $\phi$  for various elastic properties of the slab and the basal layer. For slope angles below 55° the contribution due to bending cannot be neglected. For angles below 40° the component due to bending was higher than the shear component for the evaluated snow properties, except in the case with a high Young’s modulus for the slab and a low one for the basal layer.

**4. Discussion**

**4.1. Failure Behaviour**

[15] Three evidences were found that the failure observed in the tests was a fracture process driven by stress concen-

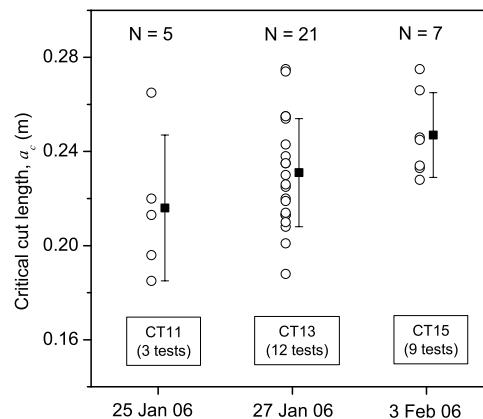


**Figure 3.** Critical cut length  $a_c$  on the three test days. The mean values and standard deviations are indicated by the squares. Median compression test (CT) scores and number of compression tests are indicated at the bottom.

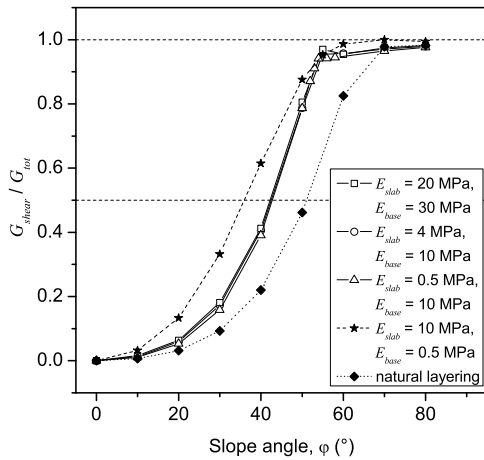


**Figure 4.** The ratio of the energy release rate due to shear deformation  $G_{shear}$  to the energy release rate due to shear and bending of the slab  $G_{tot}$  is plotted in relation to the slope angle  $\varphi$  for various elastic properties of the slab and the basal layer. In the last case (diamonds) the slab consisted of several layers with elastic and geometric properties as measured in the field tests.

trations at the crack tip and not a global failure of the weak layer due to shear stresses exceeding shear strength. First, the measured shear strength was in all tests more than three times higher than the shear stress applied on the remaining area of the weak layer. Second, in some occasions in which the weak layer did not fail entirely, the slab failed in a tensile failure ahead of the saw position, providing evidence that a fracture had propagated in the weak layer, generally between 20 cm and 50 cm. Third, snow blocks of different length  $l$  failed at the same critical cut length  $a_c$  (at least if  $l$  was larger than about  $2a_c$ ). Since blocks of different length were tested within meters on the same slope and at the same day, the differences in layer properties for the blocks can be neglected. A global failure can definitely be excluded, since for an unchanged loading situation the failure area doubled or even tripled for the different block lengths.

#### 4.2. Critical Energy Release Rate

[16] The mean critical energy release rate of  $G_c = 0.07 \pm 0.02 \text{ J m}^{-2}$  that was found for the tested weak layer on 27 January 2006, is comparable to the critical energy release rate found in previous laboratory experiments ( $G_c = 0.04 \pm 0.02 \text{ J m}^{-2}$ ) [Sigrist *et al.*, 2006]. Compared to critical energy release rates for interfaces such as ice-aluminum ( $G_c = 1 \text{ J m}^{-2}$ ) or ice-steel ( $G_c = 5 \text{ J m}^{-2}$ ) [Wei *et al.*, 1996], the above values for weak snowpack layers are extremely low. This coincides with other findings for snow, such as the very low fracture toughness in mode I [e.g., Sigrist *et al.*, 2005].  $G_c$  was independent of the block length, as it is expected as long as the block length is much larger than the size of the fracture process zone, which is about 5 cm for snow [Sigrist, 2006]. For shorter blocks than used in our experiments, Gauthier and Jamieson [2006a] found a dependence of the critical cut length on the block length.

[17] Based on the model by Heierli and Zaiser [2006] the critical failure size required to start fracture propagation along a weak layer in a snow cover on an undisturbed slope

can be estimated. The failure size is expected to be about 2.5 times larger than the critical cut length in our experiments, i.e. in the order of several decimetres [Sigrist, 2006].

#### 4.3. Slope Normal Bending

[18] The FEM results showed that bending contributed a considerable amount of energy to the available energy for crack propagation. These findings correspond well with the analytical model of Heierli and Zaiser [2006]. In order to replace the FE simulations by an analytical solution in the future, it should be considered that a potential analytical solution [such as Heierli and Zaiser, 2006] is easier to adapt to a rectangular test geometry, similar to Figure 2b.

[19] Figure 4 shows that for slope angles lower than about  $45^\circ$ , i.e. in the relevant slope angle range for snow avalanche release, more than 50% of the energy was contributed by slope normal bending in our test setup. The small kinks in the curves at a slope angle of about  $55^\circ$  originated from an opening moment in mode I of the crack due to a deformation of the whole snow block (especially for slabs with a low Young's modulus) which seemed to increase the shear contribution. However, this effect was a result of the limited extensions of our snow blocks and will have no relevance in a real slope.

[20] According to Figure 4, the critical energy release rate to fracture a weak layer can easier be exceeded if not only a slope parallel shear deformation contributes to the available energy for crack propagation but also a deformation due to slope normal bending. Slope normal bending might also contribute to crack propagation during slab release if a weak layer collapses over a certain area. However, due to contact between slab and crushed weak layer the energy contribution might be smaller than in the case of free bending. On the other hand friction between the layers will reduce the contribution due to slope parallel shear deformation.

#### 5. Conclusions

[21] The critical energy release rate of a weak snowpack layer was for the first time measured with in-situ field experiments. The proposed field test is suited to assess the conditions for crack propagation. The measured critical cut length—integrating weak layer and slab properties—indicates the failure size needed to start a self-propagating fracture. The thereof calculated critical energy release rate is equivalent to the energy needed to fracture a unit area of the weak layer.

[22] Whereas the energy that has to be exceeded to fracture a weak layer depends only on the material properties of the weak layer, the energy that is available for crack propagation depends mainly on the material properties of the overlying slab and the slope normal collapse height of a weak layer.

[23] The critical energy release rate was determined to  $G_c = 0.07 \pm 0.02 \text{ J m}^{-2}$ . Both, higher and lower values of  $G_c$  are expected to be found for different types of weak snowpack layers. A critical cut length of about 25 cm was required to start fracture propagation in the tested weak layers (mainly faceted crystals) suggesting that the critical failure size required to start fracture propagation along a weak layer in a snow cover on an undisturbed slope is in the order of several decimetres.

[24] Finite element simulations based on our field experiments showed that bending of the slab in slope normal direction contributed considerably to the energy release rate  $G$  and even dominated the component due to slope parallel shear deformation for slope angles below  $45^\circ$ . Bending in slope normal direction can be the result of a gap induced by a snow saw but could also be the result of a collapse of the weak layer. It is suggested that also in the case of dry-snow slab avalanche release bending might be an additional energy source for fracture propagation.

[25] **Acknowledgments.** We would like to thank Joachim Heierli, Jürg Dual and Hans-Jakob Schindler for valuable discussions.

## References

- Bažant, Z. P., G. Zi, and D. McClung (2003), Size effect law and fracture mechanics of the triggering of dry snow slab avalanches, *J. Geophys. Res.*, *108*(B2), 2119, doi:10.1029/2002JB001884.
- Colbeck, S. C., E. Akitaya, R. Armstrong, H. Gubler, J. Lafeuille, K. Lied, D. McClung, and E. Morris (1990), The international classification of seasonal snow on the ground, 23 pp., Int. Comm. on Snow and Ice, Int. Assoc. of Hydrol. Sci., Wallingford, U. K.
- Faillietaz, J., D. Daudon, D. Bonjean, and F. Louchet (2002), Snow toughness measurements and possible applications to avalanche triggering, in *Proceedings of the International Snow Science Workshop 2002, Penticton BC, Canada, 29 September–4 October 2002*, edited by J. R. Stevens, pp. 40–543, Int. Snow Sci. Workshop Can., Victoria, B. C., Canada.
- Fyffe, B. (2006), Mechanisms of snow slab avalanche release, Ph.D. thesis, Univ. of Edinburgh, Edinburgh, U. K.
- Gauthier, D., and J. B. Jamieson (2006a), Evaluating a prototype field test for weak layer fracture and failure propagation, in *Proceedings of the International Snow Science Workshop 2006, Telluride CO, U. S. A., 1–6 October 2006*, edited by J. A. Gleason, pp. 107–116.
- Gauthier, D., and J. B. Jamieson (2006b), Towards a field test for fracture propagation propensity in weak snowpack layers, *J. Glaciol.*, *52*(176), 164–168.
- Heierli, J., and M. Zaiser (2006), An analytical model for fracture nucleation in collapsible stratifications, *Geophys. Res. Lett.*, *33*, L06501, doi:10.1029/2005GL025311.
- Jamieson, J. B. (1999), The compression test—After 25 years, *Avalanche Rev.*, *18*(1), 10–12.
- Johnson, J. B., and M. Schneebeli (1999), Characterizing the microstructural and micromechanical properties of snow, *Cold Reg. Sci. Technol.*, *30*(1–3), 91–100.
- Kirchner, H. O. K., G. Michot, and T. Suzuki (2000), Fracture toughness of snow in tension, *Philos. Mag. A*, *80*(5), 1265–1272.
- McClung, D. M. (1979), Shear fracture precipitated by strain softening as a mechanism of dry slab avalanche release, *J. Geophys. Res.*, *84*(B7), 3519–3526.
- McClung, D. M. (1981), Fracture mechanical models of dry slab avalanche release, *J. Geophys. Res.*, *86*(B11), 10,783–10,790.
- Mellor, M. (1975), A review of basic snow mechanics, in *Symposium at Grindelwald 1974—Snow Mechanics, IAHS Publ.*, *114*, 251–291.
- Palmer, A. C., and J. R. Rice (1973), The growth of slip surfaces in the progressive failure of over-consolidated clay, *Proc. R. Soc. London, Ser. A*, *332*, 527–548.
- Schweizer, J., J. B. Jamieson, and M. Schneebeli (2003), Snow avalanche formation, *Rev. Geophys.*, *41*(4), 1016, doi:10.1029/2002RG000123.
- Schweizer, J., G. Michot, and H. O. K. Kirchner (2004), On the fracture toughness of snow, *Ann. Glaciol.*, *38*, 1–8.
- Sigrist, C. (2006), Fracture mechanical properties of snow and application to dry snow slab avalanche release, Ph.D. thesis, Swiss Fed. Inst. of Technol., Zurich, Switzerland.
- Sigrist, C., J. Schweizer, H. J. Schindler, and J. Dual (2005), On size and shape effects in snow fracture toughness measurements, *Cold Reg. Sci. Technol.*, *43*(1–2), 24–35.
- Sigrist, C., J. Schweizer, H. J. Schindler, and J. Dual (2006), The energy release rate of mode II fractures in layered snow samples, *Int. J. Fract.*, *139*(3–4), 461–475.
- Simenhois, R., and K. W. Birkeland (2006), *Proceedings of the International Snow Science Workshop 2006, Telluride CO, U. S. A., 1–6 October 2006*, edited by J. A. Gleason, pp. 79–85.
- Wei, Y., R. M. Adamson, and J. P. Dempsey (1996), Ice/metal interfaces: Fracture energy and fractography, *J. Mater. Sci.*, *31*, 943–947.

J. Schweizer and C. Sigrist, WSL Swiss Federal Institute for Snow and Avalanche Research, CH-7260 Davos, Switzerland. (schweizer@slf.ch)